

Optimizing a spin-flip Zeeman slower

L. Zhao,* J. Jiang, and Y. Liu

Department of Physics, Oklahoma State University, Stillwater, OK 74078

We present a design of a spin-flip Zeeman slower controlled by a fast feedback circuit for a sodium Bose-Einstein condensate apparatus. We also demonstrate how the efficiency of the slower strongly depends on its intrinsic parameters, and compare these observations with a few theoretical models. Our findings lead to a simple three-step procedure of designing an optimal Zeeman slower for neutral atoms, especially for those atomic species with high initial velocities, such as sodium and lithium atoms.

PACS numbers: 020.3320, 020.7010, 020.7490, 020.0020

I. INTRODUCTION

Laser cooling and trapping neutral atoms with a magneto-optical trap (MOT) has become an important step in a successful production of ultracold quantum gases [1]. To improve the capture efficiency of a MOT, a number of slowers were invented to slow hot atoms before they overlap with the MOT [1–6]. Atoms and a resonant laser beam counter propagate in a slower. The longitudinal velocity and corresponding Doppler shift of these atoms decrease after they absorb resonant photons. After a few such absorptions, these slowed atoms are no longer resonant with the laser beam and thus cannot be further slowed down. In order to continuously slow atoms along the laser beam path, one can vary the laser frequency accordingly as with the frequency chirp method [7] or by using broadband lasers [8]. Another widely-used method is to compensate differences in the Doppler shift with a spatially varying magnetic field generated by a Zeeman slower while keeping the laser frequency unchanged [1, 3–5, 9–13]. In this paper, we present the design and construction of a spin-flip Zeeman slower controlled by a fast feedback circuit for a sodium Bose-Einstein condensate (BEC) apparatus. An efficient method of optimizing a slower with our simulation program and by monitoring the number of atoms trapped in the MOT is also explained. In addition, our data demonstrates how the efficiency of a slower strongly depends on a few of its intrinsic parameters, such as the intensity of the slowing laser beam and the length of each section in the slower. These findings result in a simple three-step procedure of designing an optimal Zeeman slower for neutral atoms, especially for those atomic species with high initial velocities, for example lithium atoms.

II. EXPERIMENTAL SETUP

A sodium beam is created by an oven consisting of a half nipple and an elbow flange. A double-sided flange

with a 6 mm diameter hole in the center is used to collimate the atomic beam. To collect scattered atoms, a cold plate with a 9 mm diameter center hole is placed before a spin-flip Zeeman slower and kept at 10 °C with a Peltier cooler. Our multi-layer slower has three different sections along the x axis (i.e., a decreasing-field section, a spin-flip section, and an increasing-field section), as shown in Fig. 1(a). Compared with the single-layer Zeeman slower with variable pitch coils [11], this multi-layer design provides us enormous flexibilities in creating large enough B for slowing atoms with high initial velocities (e.g., sodium and lithium atoms). The first section of our Zeeman slower produces a magnetic field with decreasing magnetic field strength B . We choose $B \sim 650$ Gauss at the entrance of the slower, so the slowing beam only needs to be red-detuned by δ of a few hundred MHz from the D2 line of ^{23}Na atoms. This frequency detuning is easily achieved with an acousto-optic modulator, but is still large enough to avoid perturbing the MOT. The spin-flip section is simply a bellow as to maintain $B = 0$ for atoms to be fully re-polarized and also to damp out mechanical vibrations generated by vacuum pumps. The increasing-field section creates a magnetic field with increasing B but in the opposite direction to that of the decreasing-field section, which ensures the magnetic field quickly dies off outside the slower. This slower can thus be placed close to the MOT, which results in more atoms being captured. The MOT setup is similar to that of our previous work [14] and its maximum capture velocity v_c is ~ 50 m/s.

To precisely adjust B inside the slower, all layers of magnetic coils are divided into four groups, and different layers in each group are connected in series and controlled by one fast feedback circuit. A standard ring-down circuit consisting of a resistor and a diode is also connected in parallel with each coil for safely shutting off the inductive current in the coil. An important chip in our control circuit is a high power metal oxide semiconductor field effect transistor (MOSFET) operated in the linear mode. We use a number of MOSFETs connected in parallel and mount them on the top of a water-cooled cold plate to efficiently cool them. A carefully chosen resistor R_s of 50 m Ω is connected to each MOSFET's source terminal to encourage equal current splitting among the MOSFETs in parallel. R_s also limits MOSFET's transcon-

* lichao@okstate.edu

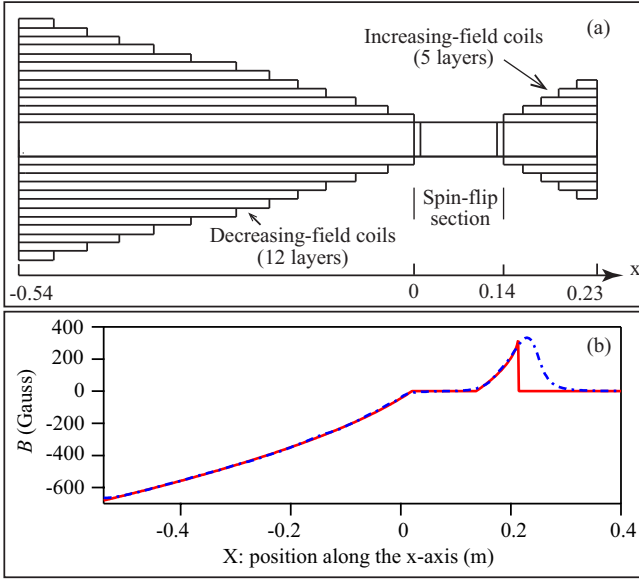


FIG. 1. (color online) (a) schematic of our spin-flip Zeeman slower. The first layer of the decreasing-field coils has 188 turns and its length is 0.54 m. The second layer is 0.51 m long and wrapped on the surface of the first layer. Similarly, the following layers are wrapped on the surface of its corresponding previous layer. The increasing-field section has five layers and is constructed in a similar way. All axes are not to scale. (b) A comparison between a theoretical prediction (solid red line) and the performance of our optimized Zeeman slower (dash-dotted blue line), with $\delta = -512$ MHz and η in decreasing- and increasing-field sections being set at 0.65. Atoms propagate along the positive x -axis direction. The MOT center locates at 0.45 m, where residual magnetic fields created by the slower are negligible.

ductance to a narrow range, which enables our feedback circuit to control both low and high electric currents with a single set of gains. The design of this feedback circuit is available upon request.

III. OPTIMIZATION

When neutral atoms pass through the Zeeman slower, only those atoms with a longitudinal velocity $v(x) = -[2\pi\delta + \mu B(x)/\hbar]/k$ are resonant with the slowing beam and can be slowed. Here μ is the magnetic moment, \hbar is the reduced Planck's constant, k and δ are the wavevector and frequency detuning of the laser beam, respectively. The actual deceleration $a_s = \eta a_{\max}$ in the slower is thus given by

$$\frac{dB(x)}{dx} = -a_s \frac{\hbar k}{\mu v} = \eta a_{\max} \frac{\hbar k^2}{\mu[2\pi\delta + \mu B(x)/\hbar]}, \quad (1)$$

where η is a safe factor to account for magnetic field imperfections in a given slower and the finite intensity of the slowing laser beam, and $a_{\max} = \hbar k \Gamma / 2m$ is the maximal achievable deceleration. m and Γ are the mass

and the natural linewidth of the atoms, respectively.

Our largest MOT is achieved when we match $B(x)$ inside the slower as precisely as possible to a prediction derived from Eq. 1 with η being set at 0.65 in decreasing- and increasing-field sections and $v_f = 40$ m/s, as shown in Fig. 1(b). Here v_f is the velocity of atoms at the end of the slower. N , the number of atoms in a MOT, can also be boosted by a larger atomic flux with a hotter atomic oven. However, this is generally not a favorable method due to two reasons. First, a hotter oven generates atoms with higher initial average velocities, but a slower can only handle entering atoms of a certain maximum velocity. Second, alkali metals' consumption rates sharply increase with the oven temperature.

We find that convenient parameters to adjust are slowing beam's intensity I and frequency detuning δ , electric current i in each magnetic coil, and the length of each section of the slower. These parameters, however, cannot be optimized independently since there is a strong correlation among them. In order to efficiently optimize the slower, we developed a computer program to simulate $B(x)$ and compared the simulation results to the actual magnetic field strengths in the slower under many different conditions (e.g., at various values of i). The actual magnetic field strengths were measured with a precise Hall probe before the slower was connected to the vacuum apparatus. The agreements between the simulation results and the measurements are good, i.e., the discrepancies are $< 5\%$. This simulation program can thus mimic the actual performance of a Zeeman slower and provide a reasonable tuning range for each aforementioned parameter, which allows for efficiently optimizing the slower. Our simulation program is available upon request.

One common way to evaluate a slower's performance is from knowing the exact number of atoms whose velocities are smaller than v_c with a costly resonant laser. In the next four subsections, we show that a convenient detection method of optimizing a slower is to monitor the number of atoms captured in the MOT, i.e., more atoms trapped in a given MOT setup indicate a better performance of the slower.

A. Intensity of the slowing beam

Figure 2 shows that the MOT capture efficiency strongly depends on the slowing beam power P , i.e., N increases with P and then stays at its peak value N_{\max} when P is higher than a critical value. This can be understood from the relationship between the safe factor η of a slower and the slowing beam intensity I . Based on Ref. [13], the safe factor η_{laser} at a finite I can be expressed as,

$$\eta_{\text{laser}} = \frac{I/I_s}{1 + I/I_s + [\frac{2\pi\delta + \mu B/\hbar + kv}{\Gamma/2}]^2} \leq \eta_{\text{laser}}^{\max} = \frac{I/I_s}{1 + I/I_s}, \quad (2)$$

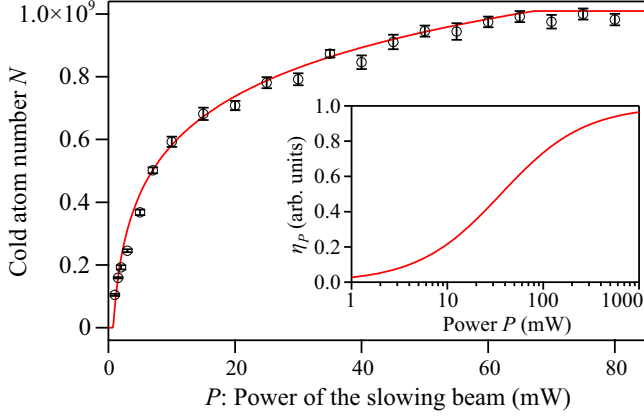


FIG. 2. (color online) N as a function of the slowing beam power P with 1 mW corresponding to $I_0/I_s = 2.5$. The solid line is a fit based on Eq. 3 with η in decreasing- and increasing-field sections being set at 0.65. Inset: η_p as a function of P for our apparatus.

where I_s is the saturation intensity of neutral atoms, e.g., it is 6.26 mW/cm² for sodium atoms. Eq. 2 implies that the safe factor of any optimal Zeeman slower has an upper limit, $\eta_{\text{laser}}^{\text{max}}$, as long as the slowing beam intensity is fixed. In other words, a bigger η in the decreasing- or increasing-field section does not always lead to a more efficient Zeeman slower if I is given.

For a Gaussian slowing beam with a width W , its intensity I can be expressed as $I(r) = I_0 \cdot e^{-\frac{2r^2}{W^2}}$. Here r is the distance away from the slowing beam center and $I_0 = 2P/(\pi W^2)$ is the beam intensity at $r = 0$. N can be given by,

$$\begin{aligned} N(P) &= \frac{N_{\text{max}}}{\pi R_0^2} \int_0^{R_0} H[\eta_{\text{laser}}^{\text{max}}(r) - \eta] 2\pi r dr \\ &= \frac{N_{\text{max}}}{R_0^2/2} \int_0^{R_0} H\left[\frac{P \cdot \exp(-\frac{2r^2}{W^2})}{\frac{\pi}{2} W^2 I_s + P \cdot \exp(-\frac{2r^2}{W^2})} - \eta\right] r dr. \end{aligned} \quad (3)$$

Here $H[r]$ is a unit step function of r to account for the fact that atoms can be efficiently slowed only when $\eta \leq \eta_{\text{laser}}^{\text{max}}(r)$, and R_0 is the radius of the atomic beam. Figure 2 shows that our data taken with $\eta = 0.65$ in decreasing- and increasing-field sections can be well fitted by Eq. 3 and N saturates at $P \geq 70$ mW. This indicates that 70 mW is the minimum power to achieve $\eta = 0.65$ for our apparatus. We can thus define a η_p , the preferred η in decreasing- and increasing-field sections at a given P , and derive its expression from Eq. 3 as follows,

$$\eta_p = P \cdot \exp(-\frac{2R_0^2}{W^2}) / [\frac{\pi}{2} W^2 I_s + P \cdot \exp(-\frac{2R_0^2}{W^2})]. \quad (4)$$

The predicted η_p as a function of P for our apparatus is shown in the inset in Fig. 2, which implies P sharply increases with η_p and is infinitely large at $\eta_p = 1$. Therefore, the first step in designing an optimal Zeeman slower

is to determine η_p from Eq. 4 based on the available slowing beam power.

B. The decreasing-field section

To focus on the decreasing-field section, our data shown in this subsection are taken with η being set at 0.65 in the increasing-field section, a fixed distance between the atomic oven and the MOT center to maintain a fixed solid angle for an atomic beam, $\delta = -512$ MHz, and $P = 70$ mW which implies η_p is 0.65. Based on the discussions in Refs. [3, 9], N can be expressed as

$$N = \int_0^{v_{\text{max}}} N_0(v) f(v) dv, \quad (5)$$

where $N_0(v) \propto v^3 e^{-\frac{mv^2}{k_B T}}$ is the initial number of atoms created by the oven, k_B is the Boltzmann constant, and the oven temperature T is set at 530 K in this work. $f(v)$ is a correction factor to account for the transverse velocity distribution of slowed atoms after they absorb resonant photons in a Zeeman slower, which can be expressed as

$$f(v) = 1 - \exp\left[-\frac{r_{\text{mot}}^2}{(v_r v/3)L^2/v_f^2}\right]. \quad (6)$$

Here r_{mot} is the radius of a MOT, L is the distance between the MOT center and the end of a Zeeman slower, v_r is the recoil velocity of an atom in a slowing process, and $\sqrt{v_r v/3}$ is the transverse velocity of slowed atoms [9]. In Eq. 5, v_{max} is the maximum velocity of entering atoms which can be handled by a slower. For a spin-flip Zeeman slower, v_{max} is given by

$$v_{\text{max}} = \sqrt{v_{\text{sf}}^2 + 2\eta_d \cdot a_{\text{max}} \cdot L_d}, \quad (7)$$

where L_d and η_d are the length and the actual safe factor of the decreasing-field section, respectively. And $v_{\text{sf}} = 2\pi\delta/k$ is the velocity of atoms which are resonant with the slowing beam at the spin-flip section, since B is zero in this section. For example, v_{sf} is 302 m/s at $\delta = -512$ MHz in our sodium BEC apparatus.

For a given δ , Eqs. 5-7 predict that N should monotonically increase with v_{max} , i.e., N increases with η_d at a fixed L_d (or N increases with L_d at a fixed η_d). However, our observations shown in Fig. 3(a) are drastically different from this prediction: at each L_d studied in this paper, N appears to first increase with η_d , reach its peak N_{max} at a critical value of η_d , and then decrease with η_d . Based on Eq. 7, we can also plot these data points as a function of v_{max} , as shown in Fig. 3(b). At each value of L_d , the agreement between our data and a theoretical prediction derived from Eqs. 5-7 (dotted black line) can only be found when v_{max} is smaller than 800 m/s, which is approximately equal to the mean velocity ($\sqrt{9\pi k_B T/8m}$) of atoms entering our slower.

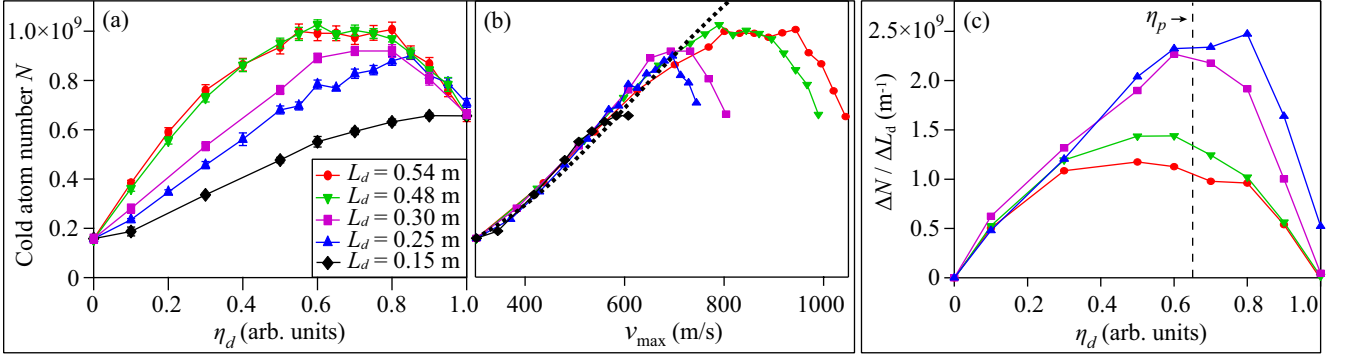


FIG. 3. (color online) N as a function of η_d (a) and v_{\max} (b) with η being set at 0.65 in the increasing-field section, $\delta = -512$ MHz, and $P = 70$ mW. Dotted black line in Panel (b) is a fit based on Eqs. 5-7. (c) $\Delta N / \Delta L_d$ as a function of η_d . Here $\Delta L_d = L_d - 0.15$ m, and ΔN is the number of extra atoms being slowed when L_d is set at a value longer than 0.15 m. Black dashed line marks the position of η_p , which is determined by the slowing laser beam power.

In addition, we plot $\Delta N / \Delta L_d$ as a function of η_d in Fig. 3(c), where $\Delta N / \Delta L_d$ represents the number of extra atoms in the MOT gained from elongating the decreasing-field section by $\Delta L_d = L_d - 0.15$ m. Figure 3(c) shows that $\Delta N / \Delta L_d$ drops to a much smaller value when L_d is increased from 0.3 m to 0.48 m. This implies the ideal length of the decreasing-field section for our apparatus should be longer than 0.3 m and shorter than 0.48 m. It is worth noting that $\Delta N / \Delta L_d$ peaks at $\eta_d \sim 0.65$ for each value of L_d , as shown in Fig. 3(c). Interestingly, the predicted η_p from Eq. 4 is also 0.65 at $P = 70$ mW, and Fig. 3(a) shows $\eta_d \sim 0.65$ is also the position where the largest N occurs. This indicates that η of our optimized decreasing-field section is actually equal to η_p . Therefore, one important procedure in designing an optimal Zeeman slower is as follows: 1) find out η_p based on Eq. 4 from the available slowing beam intensity; 2) determine the length of the decreasing-field section from Eq. 7, i.e., $L_d = [9\pi k_B T / 8m - (2\pi\delta/k)^2] / (2\eta_p a_{\max})$; 3) find out electric currents i of decreasing-field coils with our simulation program by precisely matching the simulated B to a prediction derived from Eq. 1.

C. The increasing-field section

The aforementioned discussion on the decreasing-field section applies to the increasing-field section as well. To only study the increasing-field section, data shown in this subsection are taken at $\eta_d = \eta_p = 0.65$, $L_d = 0.54$ m, and $P = 70$ mW.

Our data in Fig. 4(a) shows that N is not a monotonic function of i at a given δ . N first increases with i and reaches a peak at a critical value i_c , because a higher i leads to a larger deceleration which means more atoms can be slowed and captured in the MOT. When i is higher than i_c , we find that N sharply decreases with i due to atoms being over-slowed. Because $v_f = -(2\pi\delta + \mu B_{i\max} / \hbar) / k$, the data points in Fig. 4(a) can be converted to reveal the relationship between N

and v_f , as shown in Fig. 4(b). Here $B_{i\max}$ is the maximum magnetic field strength created by the increasing-field section at a fixed i . We find four interesting results: N always peaks around $v_f = 40$ m/s $< v_c$ at any δ within the range of -450 MHz $\leq \delta \leq -650$ MHz; the minimal

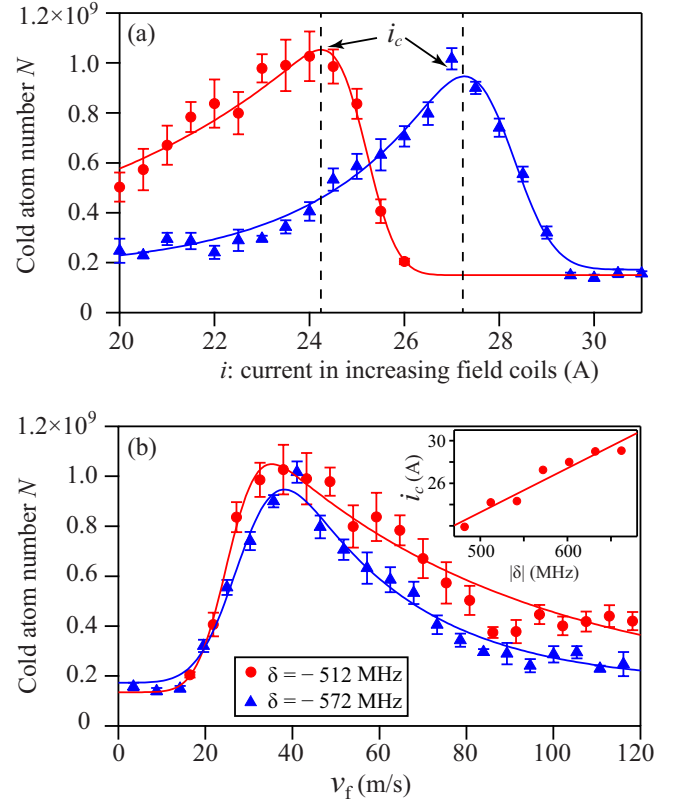


FIG. 4. (color online) N as a function of i (a) and v_f (b) at $\delta = -512$ MHz (red circles) and $\delta = -572$ MHz (blue triangles). i_c at a given δ is defined as the electric current at which N peaks. Solid lines are fits to guide the eye. Inset: i_c extracted from Panel(a) as a function of $|\delta|$. The solid line is a linear fit.

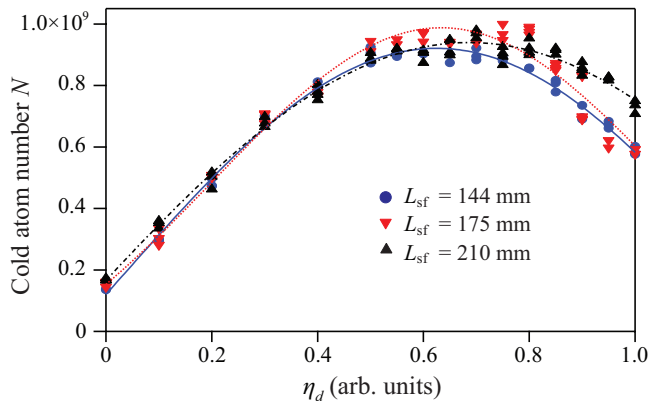


FIG. 5. (color online) N as a function of η_d at three different L_{sf} , the length of the spin-flip section (see text). Lines are Gaussian fits to the data.

velocity of the atoms captured in the MOT appears to be ~ 20 m/s; the maximum value of N does not depend on δ ; and i_c linearly increases with δ , as shown in Fig. 4. Therefore, in addition to the procedures listed in Sections 3.A and 3.B, another useful procedure in designing an optimal spin-flip Zeeman slower is as follows: 1) choose a convenient δ , for example, δ is around -500 MHz for sodium or lithium atoms; 2) find out the ideal length of the increasing-field section from the following equation, $L_i = (v_{sf}^2 - v_c^2)/(2a_s) = [(2\pi\delta/k)^2 - v_c^2]/(2\eta_p a_{\max})$; 3) determine i_c from a figure similar to Fig. 4(a) and then set the current i at a value slightly smaller than i_c in the increasing-field coils.

D. The spin-flip section

We have also studied the contribution of the spin-flip section, but have not found a strong correlation between the slower's efficiency and L_{sf} , the length of the spin-flip section. Figure 5 shows that N always peaks at $\eta_d \approx \eta_p = 0.65$ for three different values of L_{sf} , when L_d is kept at 0.54 m, η is set at 0.65 in the increasing-field section, δ is -512 MHz, and P is 70 mW. This

figure also implies that a longer spin-flip section does not boost the number of atoms captured in the MOT, as long as its length L_{sf} is sufficient to fully re-polarize atoms. A very long L_{sf} , however, has a negative effect on the MOT capture efficiency, because it also unavoidably reduces the solid angle of the atomic beam when all other parameters of the system remain unchanged.

IV. CONCLUSIONS

We have presented the design and construction of a spin-flip Zeeman slower controlled by a fast feedback circuit, and demonstrated an efficient method to optimize a slower by using our simulation program and monitoring the number of atoms trapped in the MOT. Our data suggests that an optimal Zeeman slower may be designed with the following procedures: 1) determine η_p based on Eq. 4 from the available slowing beam intensity; 2) choose a convenient δ and find out the ideal lengths of the increasing- and decreasing-field sections from $L_i = [(2\pi\delta/k)^2 - v_c^2]/(2\eta_p a_{\max})$ and $L_d = [9\pi k_B T/8m - (2\pi\delta/k)^2]/(2\eta_p a_{\max})$, respectively; 3) set i at a value slightly smaller than i_c in the increasing-field coils and determine i of decreasing-field coils with our simulation program. We have found that a longer spin-flip section does not boost the number of atoms captured in the MOT, as long as its length L_{sf} is sufficient to fully re-polarize atoms. These conclusions are very useful in designing an optimal Zeeman slower for other atomic species, especially those with high initial velocities, for example lithium atoms.

V. ACKNOWLEDGMENTS

We thank Ian Spielman and Karl Nelson for insightful discussions, and Jared Austin and Micah Webb for experimental assistances. We also thank the U. S. Army Research Office, Oklahoma Center for the Advancement of Science and Technology, and Oak Ridge Associated Universities for financial support.

-
- [1] H. Metcalf and P. Van Der Straten, *Laser Cooling and Trapping*, Graduate Texts in Contemporary Physics (Springer, 1999).
 - [2] W. Ketterle, K. B. Davis, M. A. Joffe, A. Martin, and D. E. Pritchard, "High densities of cold atoms in a dark spontaneous-force optical trap," *Phys. Rev. Lett.* **70**, 2253–2256 (1993).
 - [3] D. Durfee, "Dynamic properties of dilute bose-einstein condensation," Ph.D. thesis, Massachusetts Institute of Technology (1999).
 - [4] W. D. Phillips and H. Metcalf, "Laser deceleration of an atomic beam," *Phys. Rev. Lett.* **48**, 596–599 (1982).
 - [5] D. S. Naik, "Bose-einstein condensation: Building the testbeds to study superfluidity," Ph.D. thesis, Georgia Institute of Technology (2006).
 - [6] K. E. Gibble, S. Kasapi, and S. Chu, "Improved magneto-optic trapping in a vapor cell," *Opt. Lett.* **17**, 526–528 (1992).
 - [7] H. Wallis and W. Ertmer, "Fokker-planck analysis of atomic beam cooling by frequency chirp methods," *Journal of Physics B: Atomic, Molecular and Optical Physics* **21**, 2999 (1988).
 - [8] M. Zhu, C. W. Oates, and J. L. Hall, "Continuous high-flux monovelocity atomic beam based on a broad-

- band laser-cooling technique,” *Phys. Rev. Lett.* **67**, 46–49 (1991).
- [9] G. E. Marti, R. Olf, E. Vogt, A. Öttl, and D. M. Stamper-Kurn, “Two-element zeeman slower for rubidium and lithium,” *Phys. Rev. A* **81**, 043424 (2010).
- [10] P. Cheiney, O. Carraz, D. Bartoszek-Bober, S. Faure, F. Vermersch, C. M. Fabre, G. L. Gattobigio, T. Lahaye, D. Guéry-Odelin, and R. Mathevet, “A zeeman slower design with permanent magnets in a halbach configuration,” *Review of Scientific Instruments* **82**, 063115 (2011).
- [11] S. C. Bell, M. Junker, M. Jasperse, L. D. Turner, Y.-J. Lin, I. B. Spielman, and R. E. Scholten, “A slow atom source using a collimated effusive oven and a single-layer variable pitch coil zeeman slower,” *Review of Scientific Instruments* **81**, 013105 (2010).
- [12] C. J. Dedman, J. Nes, T. M. Hanna, R. G. Dall, K. G. H. Baldwin, and A. G. Truscott, “Optimum design and construction of a zeeman slower for use with a magneto-optic trap,” *Review of Scientific Instruments* **75**, 5136–5142 (2004).
- [13] F. Lison, P. Schuh, D. Haubrich, and D. Meschede, “High-brilliance zeeman-slowed cesium atomic beam,” *Phys. Rev. A* **61**, 013405 (1999).
- [14] J. Jiang, L. Zhao, M. Webb, N. Jiang, H. Yang, and Y. Liu, “Simple and efficient all-optical production of spinor condensates,” *Phys. Rev. A* **88**, 033620 (2013).